Adsorption (2011) 17: 211–218
DOI 10.1007/s10450-010-9316-0

Investigation on specific adsorption of hydrogen on lithium-doped mesoporous silica

Masaru Kubo · Hiroshi Ushiyama · Atsushi Shimojima · Tatsuya Okubo

Received: 5 July 2010 / Accepted: 28 December 2010 / Published online: 13 January 2011

Abstract This paper reports the synthesis, structure, and hydrogen adsorption property of Li-doped mesoporous silica (MPS) with a 2D hexagonal structure. The Li-doping is achieved by impregnation of the cylindrical mesopores with an ethanol solution of lithium chloride followed by heat treatment. Detailed characterization by solid-state NMR, TG-MS, and FT-IR suggests that, during the heat treatment, lithium chloride reacts with surface ethoxy groups (≡Si-OEt) to form ≡SiOLi groups, while ethyl chloride is released into the gas phase. The hydrogen uptake at 77 K and 1 atm increases from 0.68 wt% for the undoped MPS to 0.81 wt% for Li-doped MPS (Li-MPS). The isosteric heat of adsorption is 4.8 kJ mol^{-1}, which is consistent with the quantum chemistry calculation result (5.12 kJ mol^{-1}). The specific hydrogen adsorption on Li-MPS would be explained by the frontier orbital interaction between HOMO of hydrogen molecules and LUMO of ≡SiOLi. These findings provide an important insight into the development of hydrogen storage materials with specific adsorption sites.

Keywords Hydrogen adsorption · Li doping · Mesoporous silica · Quantum chemistry calculation

1 Introduction

Hydrogen is important as a clean, renewable energy source with high energy density (Schlapbach and Züttel 2001). To realize a hydrogen-based fuel economy, a safe and efficient method of hydrogen storage is required. Physisorption of hydrogen on porous solids such as carbon, metal-organic frameworks (MOFs), and zeolites have attracted special attention because fast kinetics and reversibility of adsorption are expected. The major drawback of the physisorption is the low adsorption uptake due to the weak interactions with hydrogen molecules. The isosteric heat of adsorption of hydrogen on porous materials is reported to be 5–10 kJ mol^{-1} (Murray et al. 2009; Jhung et al. 2007), whereas Lochan et al. proposed that the magnitude of ideal binding energy should be in the range of 20 to 40 kJ mol^{-1} for physisorption of hydrogen at 298 K (Lochan and Head-Gordon 2006). To enhance the interaction between hydrogen molecules and adsorbents, it is essential to incorporate specific adsorption sites that have strong binding energies to hydrogen molecules (Belof et al. 2007).

Alkali metal cations are known to act as adsorption sites that interact with hydrogen without dissociation, as suggested by theoretical (Barbatti et al. 2001; Vitillo et al. 2005) and experimental (Wu 1979; Bushnell et al. 1994) investigations. In particular, Li cation has a strong binding energy to hydrogen molecules (7.8 to 22.6 kJ mol^{-1}) (Barbatti et al. 2001). Goddard group reported that Li-doping into carbon materials and MOFs could increase the hydrogen uptake up to 6.0 wt% at 273 K and 100 bar by theoretical investigation (Han and Goddard 2007, 2008; Han et al. 2007). Experimentally, Hupp group succeeded in Li-doping into MOF by framework reduction through direct contact of MOFs with solid alkaline metals (Mulfort and Hupp 2007, 2008; Mulfort et al. 2009). The Li cation can be also introduced to the anionic sites of MOFs by ion exchange reactions (Nouar et al. 2009; Himsl et al. 2009; Yang et al. 2008). These methods for Li-doping can increase the hydrogen uptake and isosteric heat of adsorption, but require special organic linkers to be integrated in the frameworks.

M. Kubo · H. Ushiyama · A. Shimojima · T. Okubo (✉)
Department of Chemical System Engineering,
The University of Tokyo, 7-3-1 Hongo, Bunkyo-ku,
Tokyo 113-8656, Japan
e-mail: okubo@chemsys.t.u-tokyo.ac.jp

Recently, we reported a facile method for the Li-doping of ordered mesoporous silica (MPS) by impregnation of the mesopores with an ethanol solution of lithium chloride followed by heat treatment (Chino et al. 2005). During heating above 673 K, Cl anion was released in the form of ethyl chloride, leaving Li cations in the mesopores. Interestingly, reversible adsorption of hydrogen on Li-MPS was observed at room temperature under atmospheric pressure; the adsorbed amount of hydrogen became 4–5 times larger than that on non-doped MPS. Based on ESR analysis, unpaired electrons trapped on the silica surface were assumed to be specific adsorption sites for hydrogen molecules. This assumption is, however, inconsistent with the previous reports that the hydrogen adsorption on surface dangling bonds or defects of carbon (Orimo et al. 1999), boronnitride (Tang et al. 2002), or carbonnitride (Ohkawara et al. 2003) materials are generally irreversible. Further investigations are necessary for deeper understanding of the mechanism of specific hydrogen adsorption property of Li-MPS.

In this paper, detailed studies of the structure and surface character of Li-MPS, reaction path during heat treatment, and hydrogen adsorption capability at 77 and 87 K are presented. The presence of ethoxy (≡SiOEt) groups on silica surface is found to be essential for Li-doping, and an efficient doping is achieved by promoting surface esterification during the impregnation step, i.e., by simply increasing the temperature. Based on the experimental results, a model on the surface of Li-MPS is constructed and their interaction with hydrogen molecules is investigated by quantum calculation.

2 Method

2.1 Sample preparation

Mesoporous silica (MPS) was prepared by hydrolysis of silicon alkoxide in the presence of cationic surfactants under acidic conditions. Tetraethoxysilane ($(C_2H_5O)_4Si$, abbreviated as TEOS) was mixed with an acidic aqueous solution of hexadecyltrimethylammonium bromide ($CH_3(CH_2)_{15}N(CH_3)_3Br$, abbreviated as CTAB), and the mixture was stirred for 2.5 min at room temperature. The molar ratio of the reactants was TEOS:CTAB:H_2O:HCl = 0.10:0.11:100:8.0 (Miyata et al. 2002). After the reaction at 353 K for 2 days, precipitates were recovered by filtration, washed with distilled water, and dried at 333 K. Calcination of the as-synthesized samples was conducted in an air atmosphere in a muffle furnace at 813 K for 6 h at a heating rate of 2 K min^{-1}. For Li-doping, MPS was refluxed at ca. 353 K in a saturated LiCl/ethanol solution under N_2 atmosphere for 1 day, followed by filtration and drying in air for overnight (denoted as LiCl-MPS) (Chino et al. 2005). Li-MPS was obtained by heating LiCl-MPS at 773 K at heating rate of 4 K min^{-1} for 4 h in argon flow (100 cm^3 min^{-1}).

2.2 Characterization

Powder X-ray diffraction (XRD) measurements were performed using M03X-HF22 (Mac Science Co.) equipped with a Cu Kα radiation source (wavelength of 0.15406 nm). Nitrogen adsorption–desorption measurement at 77 K and hydrogen adsorption measurement at 77 and 87 K were performed using AUTOSORB-1 (Quantachrome Co.). The samples were pre-treated at 573 K for 8 h under vacuum. Specific surface areas were calculated by the Brunauer–Emmett–Teller (BET) method. Pore size distributions were calculated from the adsorption branch by the Barrett–Joyner–Halenda (BJH) method. Fluorescent X-ray spectroscopy (XRF) measurement was performed using a JEOL JSX-3200 at 5–30 kV and 0.0125–0.3 mA under vacuum for the quantitative analysis of chloride. The inductively coupled plasma atomic emission spectrometry (ICP-AES) measurement was performed using P4010 (Hitachi) for the quantitative analysis of Li species. The thermogravimetry-mass spectrometry (TG-MS) measurements were performed to analyze the gaseous species released from the samples during the heat treatment using a thermo gravimetric analyzer Thermoplus TG8120 (Rigaku) equipped with a mass spectrometer (Anelva). Solid-state magic-angle spinning (MAS) NMR spectra were recorded using JEOL CMX-300. ^{13}C CP/MAS NMR spectra were recorded at a resonance frequency of 75.57 MHz with a contact time of 1.5 ms and a recycle delay of 5 s. ^{7}Li MAS NMR spectra were recorded at a resonance frequency of 116.79 MHz with a pulse width of 1.0 μs and a recycle delay of 5 s. Adamantane and 1.0 M LiCl solution were used as references (at 37.85 ppm and 0 ppm, respectively, relative to tetramethylsilane) for ^{7}Li and ^{13}C NMR, respectively. Fourier-transform infrared (FT-IR) spectra were obtained using Magna 560 equipped with an MCT (mercury cadmium telluride) detector at a nominal resolution of 2 cm^{-1} using wafers of samples in KBr.

2.3 Quantum chemistry calculation

In this study, density functional theory (DFT) calculation was performed using three parameter functional of Becke, Lee, Yang, and Parr commonly noted (B3LYP) (Becke 1993). Atomic orbital basis sets were used 6-31+g(d,p) for geometry optimization and frequency calculation of models, and 6-311+g(3df,2p) for single point calculation. The Gaussian 03 package (Frisch et al. 2004) was used to undertake the molecular orbital theory calculations.

3 Results and discussion

3.1 Structural characterization

Figure 1 shows the XRD patterns of MPS, LiCl-MPS, and Li-MPS. Undoped MPS exhibits three peaks that are in-

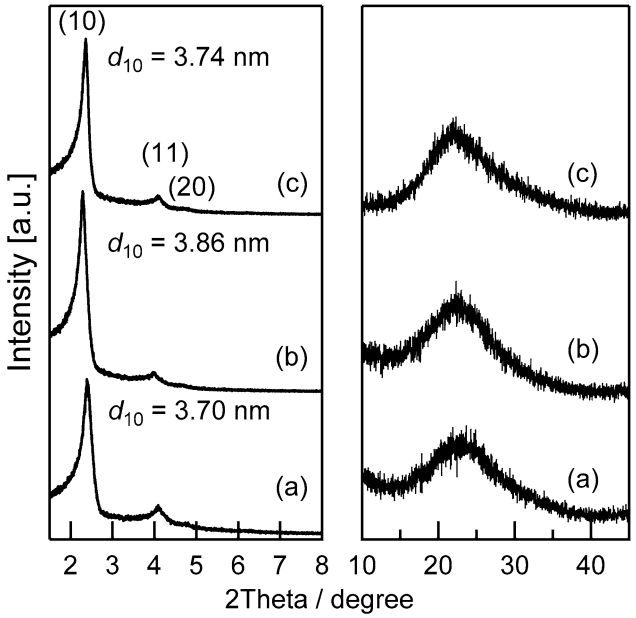

Fig. 1 Powder XRD patterns of (*a*) MPS, (*b*) LiCl-MPS, and (*c*) Li-MPS

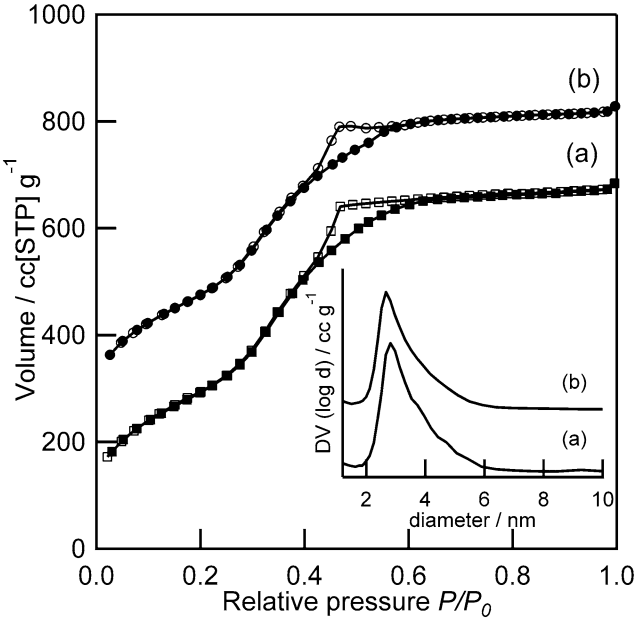

Fig. 2 Nitrogen adsorption–desorption isotherms of (*a*) MPS and (*b*) Li-MPS. The isotherm (*b*) is vertically shifted by 200 cc g^{-1}. The *filled symbols* and *open symbols* correspond to adsorption and desorption, respectively. The *inset* is BJH pore size distributions of (*a*) MPS and (*b*) Li-MPS

Table 1 Structural parameters of MPS and Li-MPS

	d_{10} *d*-spacing [nm]	Pore diameter [nm]	Wall thickness [nm]	Surface area [$m^2\,g^{-1}$]	Pore volume [$cc\,g^{-1}$]
MPS	3.70	2.8	1.43	1076	1.06
Li-MPS	3.74	2.7	1.65	1032	0.97

dexed to a 2D hexagonal structure, and no structural deterioration is observed even after LiCl impregnation and subsequent heating (Fig. 1 left). The pattern for LiCl-MPS (Fig.1(b)) shows no peak of LiCl crystals at higher angle region, implying that LiCl is well dispersed in this sample. The nitrogen adsorption–desorption isotherms of MPS and Li-MPS are shown in Fig. 2. Both are the IUPAC Type IV isotherms with hysteresis, confirming the presence of mesopores. MPS and Li-MPS have high surface areas over 1000 $m^2\,g^{-1}$ and the pore diameters of 2.8 and 2.7 nm, respectively. The structural parameters of these samples obtained from XRD and nitrogen adsorption–desorption measurements are summarized in Table 1.

The presence of Li species in these samples was confirmed by ^{7}Li MAS NMR. The spectrum of LiCl-MPS (Fig. 3(a)) shows a sharp signal at 0 ppm. This sharp signal implies that the Li species are in an isotropic state, that is, LiCl is dissolved in adsorbed water and/or residual ethanol in the mesopores rather than in the solid-state (−1.19 ppm for solid LiCl). In the spectrum of Li-MPS (Fig. 3(b)), the presence of Li species is still detected by the signal at 0.13 ppm. The signal has been slightly shifted

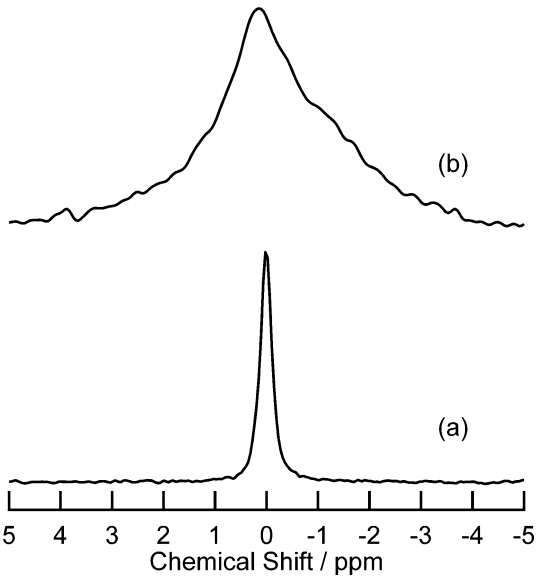

Fig. 3 Solid-state ^{7}Li MAS NMR spectra of (*a*) LiCl-MPS and (*b*) Li-MPS

and became significantly broad, suggesting that the state of Li has been changed by heat treatment. Such a broad signal is generally observed by solid-state NMR due to the chemical shift anisotropy. Unfortunately, no further information about the chemical environment of Li was obtained by ^{7}Li MAS NMR.

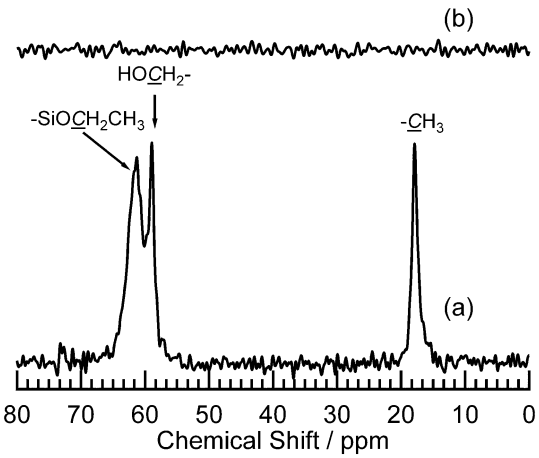

Fig. 4 Solid-state ^{13}C CP/MAS NMR spectra of (*a*) LiCl-MPS and (*b*) Li-MPS

Figure 4 shows the ^{13}C CP/MAS NMR spectra of LiCl-MPS and Li-MPS. The spectrum for LiCl-MPS (Fig. 4(a)) consists of three signals originating from ethanol used as solvent for impregnation. The sharp signals at 17.9 ppm and 58.9 ppm are unambiguously assigned to ethanol molecules (–CH_3 and $HOCH_2$–, respectively) that remained in the mesopores. The relatively broad signal at 61.3 ppm can be assigned to the ethoxy group (≡$SiOCH_2CH_3$) (Shimojima et al. 2008), confirming that surface silanol groups of MPS have been partly ethoxylated during impregnation with a LiCl/ethanol solution under reflux at 353 K. After the subsequent heat treatment at 773 K (Li-MPS), these signals disappear, indicating that both residual ethanol and ethoxy groups were mostly eliminated in LiCl-MPS (Fig. 4(b)).

3.2 Reaction during heat treatment

In our previous study on Li-doped mesoporous silica (Chino et al. 2005), it was found that ethyl chloride was released by heating at 773 K after impregnation with a LiCl/EtOH solution at room temperature. Similar result was obtained for the present LiCl-MPS sample impregnated at 353 K. Figure 5 shows the TG curve of LiCl-MPS along with the MS profiles of generated gases. LiCl-MPS was heated up to 873 K at a heat-up rate of 10 K min^{-1} under helium flow (50 cm^3 min^{-1}). The weight loss at low temperature range below ~ 423 K is attributed to the desorption of H_2O and ethanol from the mesopores. Over 773 K, significant weight loss due to the generation of ethyl chloride is observed. Considering that this temperature is much higher than the desorption temperature of free ethanol, the surface ethoxy groups rather than ethanol should play a crucial role in the formation of ethyl chloride. The resulting Li cations appeared to form a ≡SiOLi linkage, which was supported by FT-IR spectrum of Li-MPS (Fig. 6). By impregnation and

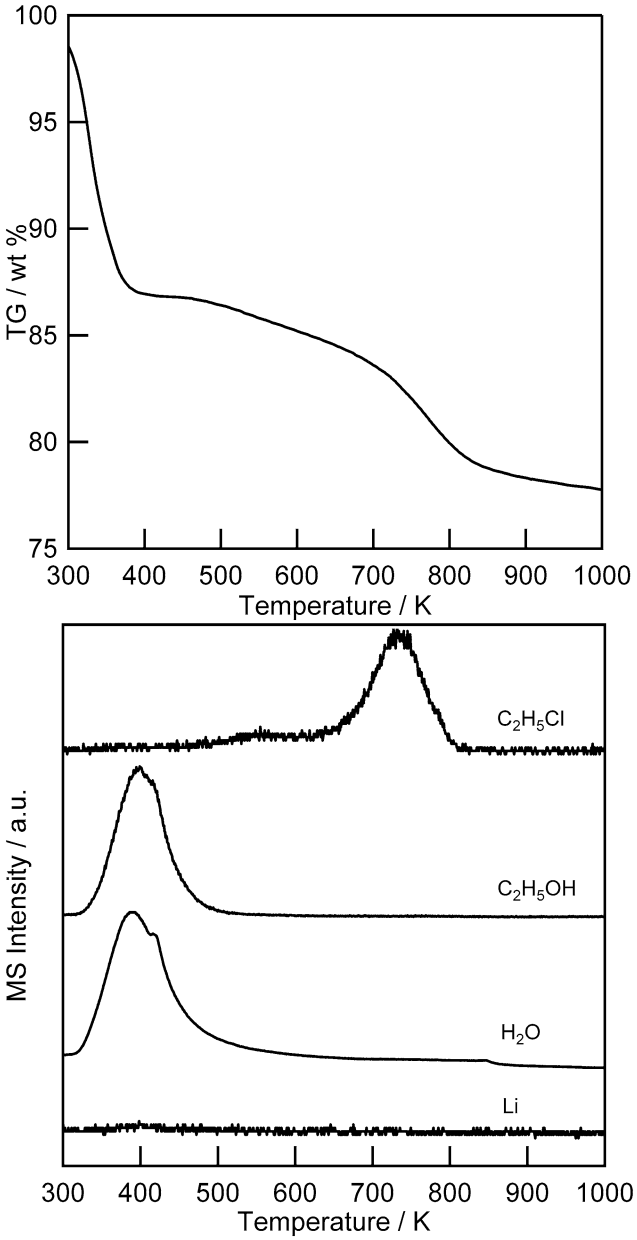

Fig. 5 (*Top*) TG curves of LiCl-MPS and (*down*) the corresponding MS profiles of the gaseous compounds produced during heating

heating, the absorption band of SiOH (969 cm^{-1}) decreases and small bands assigned to SiOLi appear at 863 cm^{-1} and 733 cm^{-1} (Park et al. 2004). From these results, the following reactions during impregnation (1) and heat treatment (2) are proposed:

$$\equiv SiOH + C_2H_5OH \rightarrow \equiv SiOC_2H_5 + H_2O \quad (1)$$

$$\equiv SiOC_2H_5 + LiCl \rightarrow \equiv SiOLi + C_2H_5Cl \quad (2)$$

It is generally known that the esterification reaction (1) is promoted at higher temperature. Therefore, the degree of esterification in the present LiCl-MPS sample should be

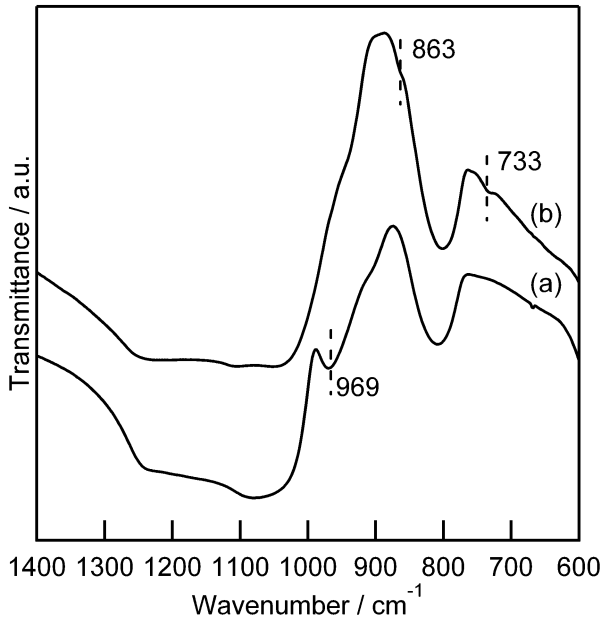

Fig. 6 FT-IR spectra of MPS (*a*) and Li-MPS (*b*)

higher than that impregnated at room temperature reported in our previous study. The increased amount of ethoxy groups should result in the increase of the ethyl chloride as well as the ≡SiOLi groups formed by the reaction (2). As shown in Fig. 7(top), in the temperature range of 500–900 K, the weight loss of LiCl-MPS impregnated at 353 K is much larger than that of the sample impregnated at room temperature. This can be attributed to the increased amount of generated ethyl chloride, as confirmed by MS spectra (Fig. 7(bottom)).

Furthermore, quantitative analyses of Li and Cl were performed by ICP-AES and XRF, respectively. The amount of Cl in LiCl-MPS impregnated at 353 K was 9.2 wt%, and 97% of Cl was released during heating. This value is higher than that reported in our previous work (40%), which is due to an increase of the amount of ethoxy groups at higher impregnation temperature. Loss of Li was not detected during heat treatment and the remained Li species was 2.27 wt%, as determined by ICP-AES. Assuming that Li is homogeneously distributed on the surface of Li-MPS, the surface density of Li species is calculated to be 1.8 ≡SiOLi per nm^2. This value is still smaller than the surface density of ≡SiOH groups of mesoporous silica (3–4 SiOH per nm^2) reported in the literature (Ramirez et al. 2003), suggesting that Li-doping would be further enhanced by increasing the amount of LiCl introduced in the mesopores, for example, by repeating the impregnation step.

3.3 Hydrogen adsorption measurement

Figure 8(left) shows the hydrogen adsorption isotherms of MPS and Li-MPS at 77 K and 87 K. At 77 K and 1 atm, the

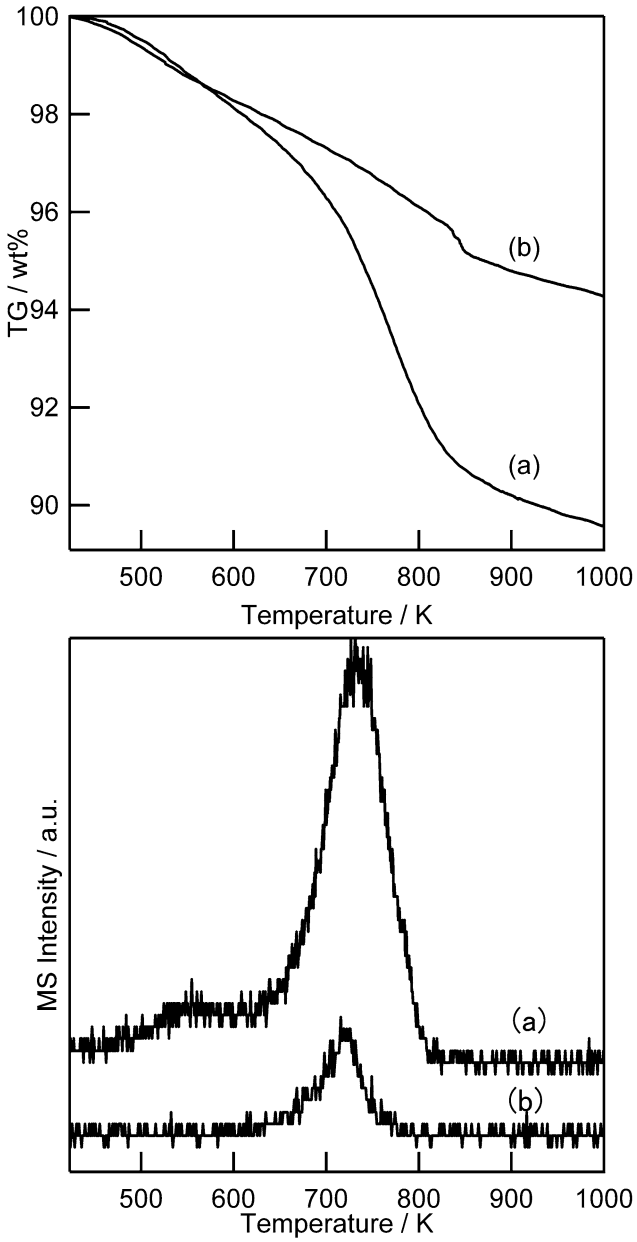

Fig. 7 (*Top*) TG curves of LiCl-MPS prepared at (*a*) 353 K and (*b*) room temperature for impregnation and (*bottom*) the MS profile of ethyl chloride

hydrogen uptakes were 0.68 wt% and 0.81 wt% for MPS and Li-MPS, respectively. The hydrogen uptake was thus increased by Li-doping. To gain some insight into the difference in the affinities with hydrogen, isosteric heats of adsorption, Q_{st}, were calculated by the Clausius-Clapeyron equation (Fig. 8(right)). In the case of undoped MPS, Q_{st} is almost constant, suggesting that the adsorption sites are homogeneously distributed on the pore surface. On the other hand, Q_{st} of Li-MPS decreases with increasing hydrogen loading. In general, hydrogen initially adsorbs on the sites with higher affinity and subsequently on other sites

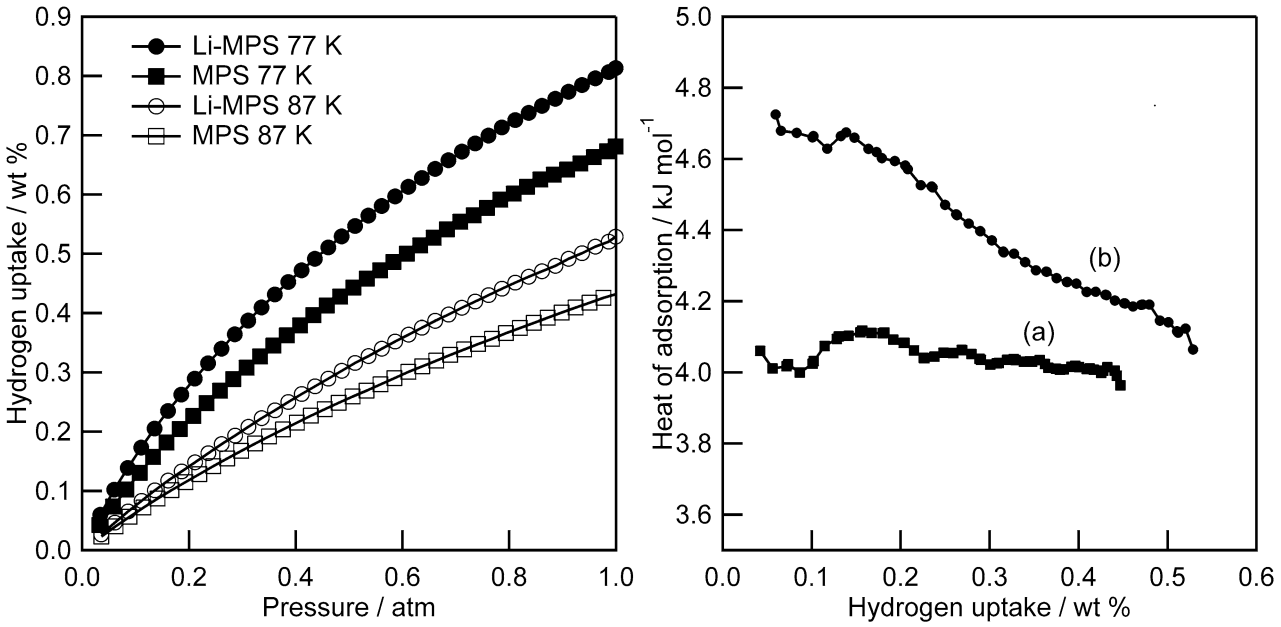

Fig. 8 (*Left*) Hydrogen adsorption isotherms of MPS (*square*) and Li-MPS (*circle*). Fills are at 77 K and blanks are at 87 K. (*Right*) Isosteric heats of adsorption for MPS (*a*) and Li-MPS (*b*)

as the pressure increases. We consider that the Li cations existing in the form of ≡SiOLi groups are acting as specific adsorption sites to increase the hydrogen uptake of Li-MPS.

3.4 Quantum chemistry calculation

The above experimental results show that Li-doping on the surface of MPS caused the enhanced hydrogen uptake by the increase of the isosteric heats of hydrogen adsorption. Here the geometry parameter, charge analysis, and interaction energies of hydrogen molecules interacting with a ≡SiOLi model are computed. First, the structure of the model system was optimized (Fig. 9(a)). The distance between the Li atom and the oxygen atom is 1.64 Å. As revealed from a natural population analysis, the Li atom has a positive charge of +0.98 |e|, and the silicon and oxygen atoms have charges of +1.28 |e| and −1.49 |e|, respectively. This means that the interaction between Li and O is ionic.

As the next step, the interaction energies of one, two, and three hydrogen molecules with this model were calculated, and their geometries were optimized as shown in Figs. 9(b), (c), and (d), respectively. The distances between the Li atom and the center of mass of the hydrogen molecule are 2.09–2.18 Å, which are the same as that reported for the Li cation and hydrogen molecules (Barbatti et al. 2001). The distance between H–H bond was elongated from 0.743 to 0.748 Å. However, this value is smaller than that reported in the literature (Barbatti et al. 2001). The binding energy of the first hydrogen molecule is 5.12 kJ mol^{-1}, which is in

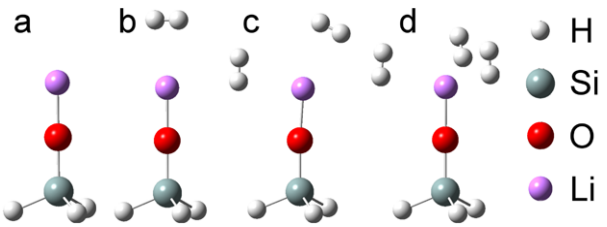

Fig. 9 Optimized geometries of the model systems: (**a**) free SiOLi group and (**b**, **c**, **d**) SiOLi groups interacting with 1, 2, and 3 H_2 molecules, respectively. The color code is as follows: *white*, hydrogen; *silver*, silicon; *red*, oxygen; *purple*, lithium

good agreement with our calculated experimental data from Fig. 8(right) (4.8 kJ mol^{-1}). When the second and third hydrogen molecules are adsorbed, the binding energy for each becomes 2.70 and 3.01 kJ mol^{-1}, respectively. For comparison, the binding energy between one hydrogen molecule and a SiOH group is −0.92 kJ mol^{-1}, confirming that the SiOH group cannot serve as a specific hydrogen adsorption site. The interaction between hydrogen molecules and ≡SiOLi can be elucidated by the so-called frontier orbital theory. The LUMO (lowest unoccupied molecular orbital) of ≡SiOLi is localized around Li atom, which is mainly found in the Li2s orbital. The orbital energy of LUMO of ≡SiOLi is approximate to that of HOMO (highest occupied molecular orbital) of hydrogen molecule. Therefore, when hydrogen molecule is adsorbed, the main interaction is derived from the HOMO of hydrogen molecules and the LUMO of ≡SiOLi, which is schematized in Fig. 10.

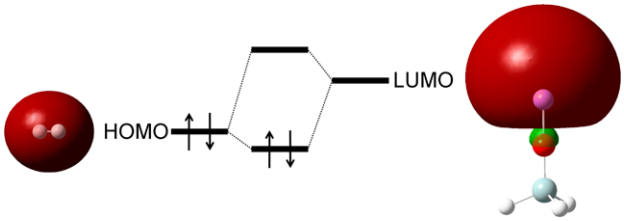

Fig. 10 Scheme of the frontier orbital interaction between hydrogen molecule and ≡SiOLi

4 Conclusions

The mechanism of specific hydrogen adsorption on Li-doped mesoporous silica was discussed based on both experimental data and quantum chemistry calculation. The adsorption sites were homogeneously distributed in undoped sample, as revealed by isosteric heat of adsorption plots. After impregnation of the mesopores with an ethanol solution of LiCl, ethoxy groups were formed on the silica surface and reacted with LiCl during heat treatment to form ≡SiOLi groups on the mesopore surface. Quantum chemistry calculation suggested that the ≡SiOLi groups bound with hydrogen molecules by the frontier orbital interaction between the HOMO of hydrogen molecules and the LUMO of ≡SiOLi. The calculated binding energy was in good agreement with the experimental data. The higher heat of adsorption on Li-MPS resulted in the enhancement of hydrogen uptake from 0.68 wt% to 0.81 wt% at 77 K and 1 atm. Note that mesoporous silica is so heavy that gravimetric density of hydrogen adsorption could not reach the practical application level (4.5 wt% by 2010, claimed by the U.S. Department of Energy (DOE)). We believe that our Li-doping method via release of anion species from lithium salts will be available for other porous materials, especially MOFs.

Acknowledgements This work was supported in part by the ENEOS Hydrogen Trust Fund and by a Grant-in-Aid for Scientific Research (B) from the Japan Society for the Promotion of Science (JSPS). M.K. acknowledges the support by a Grant-in-Aid for JSPS Fellows and Fellowship.

References

Barbatti, M., Jalbert, G., Nascimento, M.A.C.: The effects of the presence of an alkaline atomic cation in a molecular hydrogen environment. J. Chem. Phys. **114**, 2213–2218 (2001)

Becke, A.D.: A new mixing of Hartree-Fock and local density-functional theories. J. Chem. Phys. **98**, 1372–1377 (1993)

Belof, J.L., Stern, A.C., Eddaoudi, M., Space, B.: On the mechanism of hydrogen storage in a metal-organic framework material. J. Am. Chem. Soc. **129**, 15202–15210 (2007)

Bushnell, J.E., Kemper, P.R., Bowers, M.T.: $Na^+/K^+\cdot(H_2)_{1,2}$ clusters: binding-energies from theory and experiment. J. Phys. Chem. **98**, 2044–2049 (1994)

Chino, N., Ogura, M., Kodaira, T., Izumi, J., Okubo, T.: Characterization of ESR active species on lithium chloride-modified mesoporous silica. J. Phys. Chem. B **109**, 8574–8579 (2005)

Frisch, M.J., Trucks, G.W., Schlegel, H.B., Scuseria, G.E., Robb, M.A., Cheeseman, J.R., Montgomery, J.A., Jr., Vreven, T., Kudin, K.N., Burant, J.C., Millam, J.M., Iyengar, S.S., Tomasi, J., Barone, V., Mennucci, B., Cossi, M., Scalmani, G., Rega, N., Petersson, G.A., Nakatsuji, H., Hada, M., Ehara, M., Toyota, K., Fukuda, R., Hasegawa, J., Ishida, M., Nakajima, T., Honda, Y., Kitao, O., Nakai, H., Klene, M., Li, X., Knox, J.E., Hratchian, H.P., Cross, J.B., Bakken, V., Adamo, C., Jaramillo, J., Gomperts, R., Stratmann, R.E., Yazyev, O., Austin, A.J., Cammi, R., Pomelli, C., Ochterski, J.W., Ayala, P.Y., Morokuma, K., Voth, G.A., Salvador, P., Dannenberg, J.J., Zakrzewski, V.G., Dapprich, S., Daniels, A.D., Strain, M.C., Farkas, O., Malick, D.K., Rabuck, A.D., Raghavachari, K., Foresman, J.B., Ortiz, J.V., Cui, Q., Baboul, A.G., Clifford, S., Cioslowski, J., Stefanov, B.B., Liu, G., Liashenko, A., Piskorz, P., Komaromi, I., Martin, R.L., Fox, D.J., Keith, T., Al-Laham, M.A., Peng, C.Y., Nanayakkara, A., Challacombe, M., Gill, P.M.W., Johnson, B., Chen, W., Wong, M.W., Gonzalez, C., Pople, J.A.: Gaussian 03, revision C.02. Gaussian, Inc., Wallingford (2004)

Han, S.S., Goddard, W.A.: Lithium-doped metal-organic frameworks for reversible H_2 storage at ambient temperature. J. Am. Chem. Soc. **129**, 8422–8423 (2007)

Han, S.S., Goddard, W.A.: High H_2 storage of hexagonal metal-organic frameworks from first-principles-based grand canonical Monte Carlo simulations. J. Phys. Chem. C **112**(35), 13431–13436 (2008)

Han, S.S., Deng, W.Q., Goddard, W.A.: Improved designs of metal-organic frameworks for hydrogen storage. Angew. Chem. Int. Ed. **46**, 6289–6292 (2007)

Himsl, D., Wallacher, D., Hartmann, M.: Improving the hydrogen-adsorption properties of a hydroxy-modified MIL-53(Al) structural analogue by lithium doping. Angew. Chem. Int. Ed. **48**, 4639–4642 (2009)

Jhung, S.H., Yoon, J.W., Lee, S., Chang, J.S.: Low-temperature adsorption/storage of hydrogen on FAU, MFI, and MOR zeolites with various Si/Al ratios: effect of electrostatic fields and pore structures. Chem. Eur. J. **13**, 6502–6507 (2007)

Lochan, R.C., Head-Gordon, M.: Computational studies of molecular hydrogen binding affinities: the role of dispersion forces, electrostatics, and orbital interactions. Phys. Chem. Chem. Phys. **8**, 1357–1370 (2006)

Miyata, H., Noma, T., Watanabe, M., Kuroda, K.: Preparation of mesoporous silica films with fully aligned large mesochannels using nonionic surfactants. Chem. Mater. **14**, 766–772 (2002)

Mulfort, K.L., Hupp, J.T.: Chemical reduction of metal-organic framework materials as a method to enhance gas uptake and binding. J. Am. Chem. Soc. **129**, 9604–9605 (2007)

Mulfort, K.L., Hupp, J.T.: Alkali metal cation effects on hydrogen uptake and binding in metal-organic frameworks. Inorg. Chem. **47**, 7936–7938 (2008)

Mulfort, K.L., Wilson, T.M., Wasielewski, M.R., Hupp, J.T.: Framework reduction and alkali-metal doping of a triply catenating metal-organic framework enhances and then diminishes H_2 uptake. Langmuir **25**, 503–508 (2009)

Murray, L.J., Dinca, M., Long, J.R.: Hydrogen storage in metal-organic frameworks. Chem. Soc. Rev. **38**, 1294–1314 (2009)

Nouar, F., Eckert, J., Eubank, J.F., Forster, P., Eddaoudi, M.: Zeolite-like metal-organic frameworks (ZMOFs) as hydrogen storage platform: lithium and magnesium ion-exchange and H_2-(rho-ZMOF) interaction studies. J. Am. Chem. Soc. **131**, 2864–2870 (2009)

Ohkawara, Y., Kusaka, K., Ohshio, S., Higa, A., Toguchi, M., Saitoh, H.: Hydrogen storage phenomenon in amorphous phase of hydrogenated carbon nitride. Jpn. J. Appl. Phys. **42**, 5251–5254 (2003)

Orimo, S., Majer, G., Fukunaga, T., Zuttel, A., Schlapbach, L., Fujii, H.: Hydrogen in the mechanically prepared nanostructured graphite. Appl. Phys. Lett. **75**, 3093–3095 (1999)

Park, S.H., Liu, H.M., Kleinsorge, M., Grey, C.P., Toby, B.H., Parise, J.B.: [Li-Si-O]-MFI: a new microporous lithosilicate with the MFI topology. Chem. Mater. **16**, 2605–2614 (2004)

Ramirez, A., Lopez, B.L., Sierra, L.: Study of the acidic sites and their modifications in mesoporous silica synthesized in acidic medium under quiescent conditions. J. Phys. Chem. B **107**, 9275–9280 (2003)

Schlapbach, L., Züttel, A.: Hydrogen-storage materials for mobile applications. Nature **414**, 353–358 (2001)

Shimojima, A., Goto, R., Atsumi, N., Kuroda, K.: Self-assembly of alkyl-substituted cubic siloxane cages into ordered hybrid materials. Chem. Eur. J. **14**, 8500–8506 (2008)

Tang, C.C., Bando, Y., Ding, X.X., Qi, S.R., Golberg, D.: Catalyzed collapse and enhanced hydrogen storage of BN nanotubes. J. Am. Chem. Soc. **124**, 14550–14551 (2002)

Vitillo, J.G., Damin, A., Zecchina, A., Ricchiardi, G.: Theoretical characterization of dihydrogen adducts with alkaline cations. J. Chem. Phys. **122**, 114311–114319 (2005)

Wu, C.H.: Binding-energies of LiH_2 and LiH_2^+ and the ionization-potential of LiH_2. J. Chem. Phys. **71**, 783–787 (1979)

Yang, S., Lin, X., Blake, A.J., Thomas, K.M., Hubberstey, P., Champness, N.R., Schroder, M.: Enhancement of H_2 adsorption in Li^+ exchanged co-ordination framework materials. Chem. Commun. **46**, 6108–6110 (2008)